Ganesan Elizabeth Rani ✉
Marimuthu Sakthimohan
Arockiasamy Felix Sahayaraj
Mariappan Sornalakshmi

https://doi.org/10.21278/TOF.484060123
ISSN 1333-1124
eISSN 1849-1391

QUANTITATIVE AUTOMATED DETECTION OF VOIDS, PORES, CRACKS, AND FIBRE ORIENTATION IN SCANNING ELECTRON MICROSCOPY IMAGES UTILISING MASK CONVOLUTIONAL NEURAL NETWORKS (M-CNN) FOR NATURAL FIBRE COMPOSITE CHARACTERISATION

Summary

In recent years, image processing in various scientific domains has gained prominence, particularly in materials science. This study leverages advanced deep learning techniques, specifically the Mask Convolutional Neural Network (M-CNN), for quantitative analysis of Scanning Electron Microscopy (SEM) images. Our approach involves the rigorous classification of SEM images in RGB format, utilising M-CNN to intelligently scrutinise edges and quantify cracks, pores/voids, and fibre orientation. Notably, M-CNN plays a pivotal role in accurately predicting material strength by categorising angles into ductile (45°) and brittle (90°) ones. The proposed software achieves a remarkable 99% accuracy in detecting and quantifying structural elements within SEM images, marking a significant advancement in materials science and demonstrating the potential of advanced image processing techniques for material analysis.

Key words: *Deep Learning, Scanning Electron microscopy, Mask Convolutional Neural Networks (M- CNN)*

1. Introduction

Image processing serves as a fundamental and indispensable concept across a multitude of fields, offering the vital capability to glean valuable insights from visual data. The application of image processing techniques is now pervasive, enabling profound analysis of images and the extraction of pertinent information [1-3]. This technology functions in various domains, including clinical sciences, where it plays a pivotal role in the interpretation of intricate medical images such as X-ray scans and blood/cell microscopy. Moreover, it serves as a crucial tool in space science, facilitating the prediction of weather patterns, environmental conditions, and geographic mapping.

This study focuses on the domain of materials science, where the imaging of diverse composites is of paramount importance. Mechanical experts routinely employ Scanning Electron Microscopy (SEM) to capture high-resolution images of both metallic and non-metallic surfaces [4-5]. SEM-generated images serve as a valuable resource for manual assessments, particularly for factors such as cracks, voids, and fibre distribution on the surface.

However, manual assessments fall short in predicting the precise quantification of these structural elements, which significantly influence material strength [6-9].

In response to this limitation, Convolutional Neural Networks (CNNs) have emerged as a powerful tool for deep learning. CNNs exhibit unparalleled proficiency in extracting precise information from SEM images, offering the promise of automation. In particular, the Mask Convolutional Neural Network (M-CNN) is employed, leveraging RGB colour representation encompassing values within the range of 0 to 255 to execute image masking. This technique effectively segments SEM images, enabling the identification of cracks and pores, simplifying the isolation of individual objects and facilitating edge detection. This, in turn, contributes to determining material strength associated with these structural elements [10-12].

Non-metallic fibre orientation assumes a pivotal role in evaluating the stiffness and strength of composite materials, rendering it a critical parameter in their design [13-15]. Fibre orientation directly influences mechanical properties and manufacturing consistency, encompassing unidirectional, bidirectional, random, and multidirectional orientations [16]. Deep learning, featuring multiple layers, including convolutional, pooling, and fully connected layers, provides a robust approach to handling the substantial data inherent in these analyses [17-19].

This study introduces an integrated approach that capitalises on the synergy between masking techniques and M-CNN for the automated detection of tensile strength properties in fibres characterised by diverse inclinations. The foundation for accurate tensile strength estimation lies in statistical analysis, obviating the need for manual assessment and enhancing predictive capabilities. The primary objective of this endeavour is the quantitative segmentation of cracks, voids, and orientations through the amalgamation of CNN and masking, effectively addressing the intricate challenges associated with tensile strength property analysis in SEM images.

2. Background Work

In recent years, the utilisation of Convolutional Neural Networks (CNNs) has gained prominence in various scientific applications, including image analysis. Seunghwan Song et al. [20] introduced an innovative concept that embraces CNNs, particularly in the context of Spiking Neural Network (SNN) inference. Their work proposed a weight-sharing spiking CNN inference system (WS-SCNN), incorporating efficient convolution layers (ECLs) [21-23]. The key innovation here lies in the efficient mapping of convolutional features between input and filter weights, effectively reducing the hardware resources required for SNNs. Lianlin Li et al. [24] advanced the field of deep learning by combining CNNs with iterative EM inverse scattering solution techniques, giving birth to DeepNIS. This novel CNN-based solution has demonstrated superior performance in comparison to traditional inverse scattering methods, particularly in terms of image quality and processing speed.

Juanjuan Huang et al. [25] introduced an intriguing application of CNNs in the classification of M-ary phase shift keying (PSK) and M-ary quadrature amplitude modulation (QAM) modulation formats. Their approach hinged on a cascaded convolutional neural network (CasCNN) that effectively categorised various modulation formats, including PSK and QAM, demonstrating the potential for efficient digital modulation classification. Pengbo Zhang et al. [26] delved into the realm of spatial-spectral electroencephalogram (EEG) features using a novel structure called R3DCNN (a fusion of deep RNN and 3D CNN). This innovative approach exhibited impressive classification accuracy across a range of tasks, underlining its versatility and potential applications.

Zheng Liu et al. [27] pushed the boundaries of image restoration techniques with their network architecture, showcasing its potential in handling a wide array of visual distortions. Their work hinted at the prospect of future research into general-purpose image restoration

methods. Mridul Gupta et al. [28] ventured into the domain of tiny infrared target detection by integrating CNNs into an established space-based detection processing chain. Their method incorporated supervised training, utilising the sequence-to-sequence matching detection (SMD) approach, which yielded significant performance improvements. Berin Seta et al. [29] considered the impact of the fibre orientation and the strand shape's primary characteristics of the fibres (fibre volume percentage and length-to-diameter aspect ratio) [30-32]. The fibre orientation stayed the same but the cross-sectional strand form was altered for greater aspect ratio fibres and lower volume fraction (but higher anisotropy levels). A horn-like shape was created on the strand's top borders as a result of the intricate interaction between the fibre orientation and the flow that was created inside it. Zhang et al. [33] made the case that this unusual behaviour resulted from the longer fibres being printed at higher extrusion pressure and the limited sideway flow in the upper section of the strand by looking at the streamlines of the flow [34-35]. Zhihao Li and Wei Zhou [36] described how a fibre orientation device with a vibration motor with configurable vibrational frequency was employed to prepare UHPFRC. When making the gadget, the wall effect and fibre length were taken into account. To investigate the impacts of vibrational frequency and the related vibrational force on the tensile behaviours, uniaxial tensile tests were carried out on fibre-oriented UHPFRC. The test findings revealed that the UHPFRC specimens cast using the fibre orientation procedure at various vibrational frequencies had varying tensile properties.

Matteo Giardino et al. [37] explain scanning electron microscopy (SEM), where a four-quadrant backscattered electron detector (FQBSD) captures information from different angles of the sample surface. By combining these signals, researchers can create a 3D reconstruction of the surface topography. However, processing the raw data poses the significant challenge of integrating the gradient fields derived from the normalised signal difference between opposing detector pairs. Traditionally, researchers have tackled this noise-sensitive task using a least-squares integration approach, effectively averaging out inconsistencies caused by electronic noise manifested as image noise [38-41]. S.L. Lu et al. [42] describe research investigating the influence of neighbouring parent grain orientations on massive transformations in four α-β titanium alloys. The alloys were produced using three different manufacturing techniques: electron beam powder bed fusion (EB-PBF), laser directed energy deposition (L-DED), and conventional manufacturing followed by β-annealing.

These prior works in the field of deep learning, CNNs, and their diverse applications set the stage for the current study's exploration of CNN-based techniques in material science and SEM image analysis. The integration of these methodologies holds the promise of automating and enhancing the accuracy of material property assessments.

3. Proposed Methodology

3.1 Scanning Electron Microscope (SEM)

The scanning electron microscope (SEM) is a pivotal instrument in our study. SEM generates images through the interaction of high-energy electrons with the sample, resulting in secondary electrons, backscattered electrons, and characteristic X-rays. These signals are collected by detectors, forming images that are subsequently displayed on a computer screen. The penetration depth of the electron beam into the sample depends on factors like acceleration voltage and sample thickness, typically reaching depths of a few microns. This interaction leads to the generation of various signals, including secondary electrons and X-rays. Fig. 1 illustrates the process flow of our proposed methodology, where SEM images serve as the initial data, subsequently undergoing masking and analysis via a Mask Convolutional Neural Network (M-CNN) for quantitative assessment.

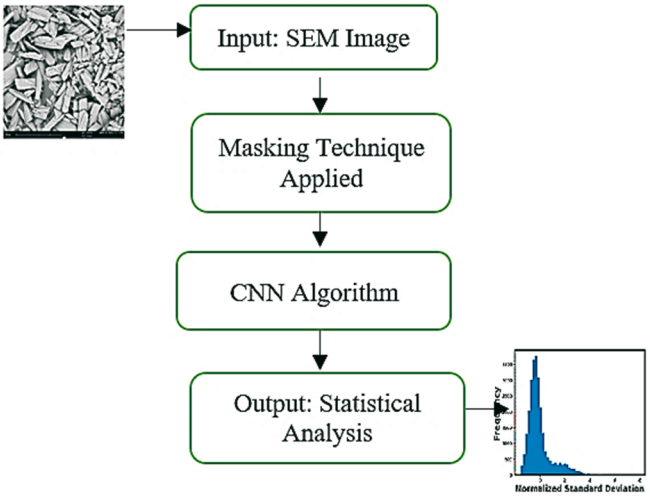

Fig. 1 Process flow of proposed methodology

3.2 Masking Technique

A critical component of our methodology is the masking technique, employed for image preprocessing. This technique plays a vital role in noise reduction and the enhancement of image features. It utilises a 3x3 box filter that segregates pixel intensities into masked and unmasked regions, assigning a value of 0 to all pixel values if they are uniform [43-44]. This approach facilitates the identification of edges within the images, ensuring smooth edge detection in cracks and pores, even at the periphery of SEM images. Pixels with varying intensities remain unchanged in the output images, allowing for easy and efficient edge detection. Table 1 illustrates the 3x3 matrix configuration of the mask.

The properties of the box filter utilised in our study are as follows:

- Odd-ordered
- Sum of all elements equals 1
- All elements are identical

Table 1 3X3 Matrix configuration of the mask

1/9	1/9	1/9
1/9	1/9	1/9
1/9	1/9	1/9

The 3x3 matrix comprises nine cells, all containing identical elements that sum to 1, thereby satisfying the required properties. This mask technique effectively facilitates the detection of cracks and pores along the image edges.

3.3 M-Convolution Neural Network (M-CNN)

The M-CNN plays a central role in our approach for structured data analysis. Fig. 2 shows the system architecture of M-CNN. Its design revolves around the incorporation of high-resolution pixel data obtained from SEM images, with pixel values ranging from 0 to 255 [45-47]. To achieve this, we developed a dataset consisting of high-resolution pixels extracted from SEM images, with each pixel represented in the range of 0 to 255, where white pixels correspond to (0, 0, 0), and black pixels to (255, 255, 255). A mask is applied to these images, preserving the Boolean values of 1 for the masked regions. This mask effectively highlights lines and voids within the SEM images.

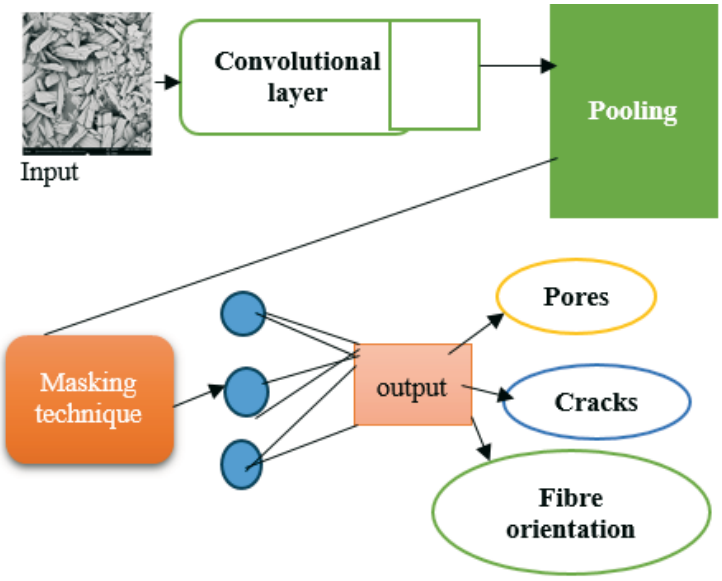

Fig. 2 System architecture of M-CNN

Different SEM images were collected for the analysis of the fibre composite images. The M-CNN architecture comprises multiple layers dedicated to feature extraction and classification. Specifically, the convolutional layers are responsible for discerning various features within the images, thereby performing feature extraction [48-50]. Numerous sets of networks consider the features extracted from the convolutional or pooling layers.

3.4 M-CNN Algorithm

The M- CNN works are explained in detail in Fig. 3. The M-CNN algorithm takes SEM images in the BGR format and converts them into the RGB format. Subsequently, the red, green, and blue values for each image are plotted in a 3D chart. The pixel points are then mapped to a range from (0, 0, 0) to (120, 120, 120), effectively optimising them for grayscale images. Through Boolean values, all pixel points from the original image are superimposed onto a single mask. The RGB colours are treated as channels, with a matrix size of six units in both height and width. A 3x3 matrix is applied as a kernel to generate convoluted images from the input SEM images.

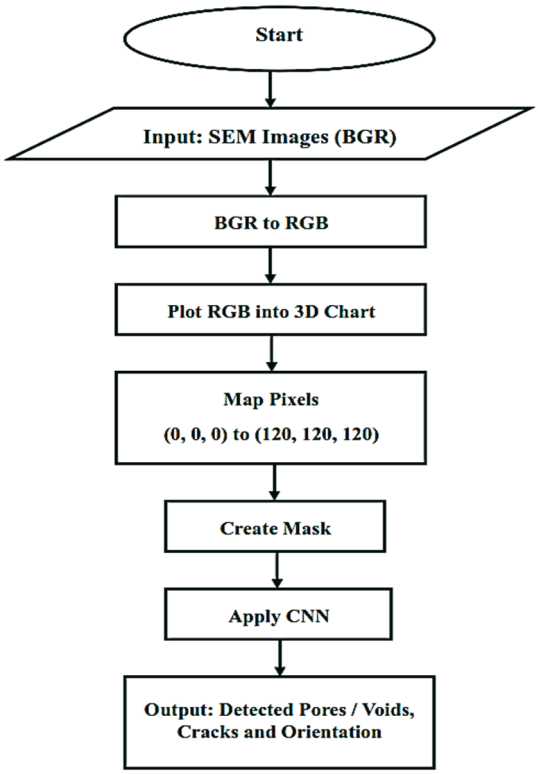

Fig. 3 M-CNN algorithm workflow

CNN Algorithm

Input: SEM image trained datasets $D_s = [\{P, C\}]$
Output: Detection of pores, cracks, and fiber orientation G_v
Masking M
for i $\{I, D_s\}$ do

find the P_n pores $\{I_o, D_o^p\} \leftarrow P$

Search the C_n cracks $\{C_o^1, D_o^p\} \leftarrow C$

for $\{n\}$ cracks, pores in $[n_{i,m}^{p}]_{m=1}^{1}$ **do**

Search the n pores $\{p_1, p_2, p_3 \ldots . p_n\} \leftarrow P$

Compute n pores features $(G_v(p_1)), (G_v(p_2)) \ldots (G_v(p_n)) * M$

Compute n cracks features $C \leftarrow (G_\phi(p_1), G_\phi(p_2) \ldots\ldots G\phi(p_n)) * M$

Compute orientation features $Gv\ (z, f_i, C_c)$

Backpropagation

end for

end for

Fig. 4 M-CNN algorithm to analyse pores, cracks and fibre orientation in SEM image

The M-CNN algorithm operates on SEM images represented as datasets (Ds) containing pairs of pores (P) and cracks (C). The algorithm shown in Fig. 4 is to detect and characterise pores, cracks, and fibre orientation (Gv). The process involves iterating through each dataset, identifying individual pores and cracks, computing their respective features, and applying backpropagation. Notably, the algorithm transforms SEM images from BGR to RGB format, optimises pixel values for grayscale, and utilises a convolutional neural network (CNN) approach with a 3x3 filter.

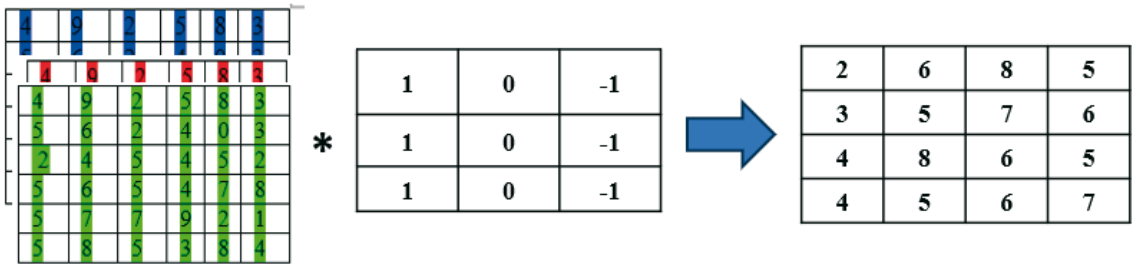

Fig. 5 Convoluted 6x6 matrix with 3x3 filter to produce results

Fig. 5 shows the convoluted 6x6 matrix with a 3x3 filter to produce the results. The output is represented as a 4x4 matrix derived from the three input channels, the filter, and the three-channel input. Nine values are obtained from each channel in the input, and the sum of 27 filter values produces the output of the corresponding element's first column. The kernel is usually a matrix of numbers and is mainly applied as part of the input which undergoes the mathematical operation called convolution. It highlights the operation of the input based on the weight value to extract features. This configuration is guided by specific features within the SEM image, with the improved characterisation algorithm aligning with user-defined parameters. It incorporates elements such as edges, attributes, pixel values, and colours, all of which contribute to defining the training dataset. The output is generated based on the input parameters, offering highly accurate identification. In cases where the alignment of Equation 1 with the input parameters is not achieved, the output is deduced from the training dataset boundaries, and the resultant difference appears as voids in the output.

$$P = I_0 - D_0 \tag{1}$$

where

P = pores estimation

I_0 = coordinating of input boundary

D_0 = dataset boundary

The accuracy of the model was assessed by comparing its predictions with real-world data. By analysing how often the model lacks important information or fails to meet the desired output (yield), we can identify areas for improvement. These weaknesses are then addressed by filling in the missing information and smoothing out any rough edges in the data. This ensures that the training data are consistent and are of high quality, which is crucial for training effective models.

This method relies on specific features identified in the SEM image. The goal is to develop an improved characterisation process that meets the client's requirements. Importantly, every location is segmented, and all data are provided to the client. This new approach significantly improves the accuracy of characterisation compared to existing methods. It takes into account edges, brightness values, and pixel intensities, all of which are crucial details used to analyse the sample data. The yield is then calculated based on these information boundaries, leading to highly precise identification. If there is no clear agreement, the input boundary can be used to infer yield based on the defined dataset boundaries. Finally, any discrepancies are identified as cracks in the yield in Equation 2:

$$C = \int C_0 - D_0 * (\mu 0 + \mu 1 + \mu 2 + \mu 3) \quad (2)$$

where

C = Cracks estimation

C_0 = coordinating of input boundary.

D_0 = dataset boundary

$\mu 0 \ldots \mu 3$ = angle calculation of four quadrants

The parameters D_0, μ0, μ1, μ2, and μ3 were determined through a combination of empirical calibration and optimisation processes. Specifically, we conducted a series of experiments and iterative adjustments to fine-tune these parameters to achieve optimal performance in our image processing methodology.

Two sets of results, 'real' and 'model predicted', were compared to see how accurate the model was. By looking at where the model lacks information or does not meet the desired outcome (yield), we can find areas where it needs improvement. These "gaps" are filled in and smoothed out (like fixing rough edges on a picture) to make the data consistent and of high quality. This is important because good training data help build better models.

3.5 Pores and Cracks Detection

In our analysis, we employ the following steps for the identification of pores, cracks, and fibre orientation:

1. Conversion of primary SEM images to binary format, representing white as 1 and black as 0.
2. Application of a bitwise AND operation between the binary image and the masked SEM image.
3. Identification of voids and pores through white regions in the SEM images.
4. Calculation of the lengths of cracks and pores based on width and perimeter.

The threshold for creating a binary image in the first step of detecting pores and cracks was determined through an adaptive thresholding technique. Specifically, we used Otsu's method, which calculates an optimal threshold based on the image histogram to maximise the variance between the foreground and background. This adaptive thresholding technique allows for effective segmentation of pores and cracks in SEM images by dynamically adjusting the threshold based on the local characteristics of the image.

3.6 Fibre Length Calculation

The M-CNN automatically computes fibre lengths in micrometres (μm) by analysing the statistical distribution of fibre diameters. This creates an important factor in the material strength and determines the number of pores and cracks present. The area of the fibre length:

$$z = \int_{l}^{u} b_0 - b_1 \tag{3}$$

where

z = SEM image area

b_0 = lower bound of pores/cracks

b_1 = upper bound of pores cracks

The lengths of the cracks/pores in the SEM images were calculated based on the width and perimeter. l is the lower limit of whether the estimated fibre length is the minimum acceptable. u is the upper limit of whether the estimated fibre length is the maximum acceptable which is shown in Equation 4:

$$f_l = (p_l/2) \cdot w_l \tag{4}$$

where

f_l = length of fibre cracks/pores

p_l = perimeter

w_l = width

The cracks/voids are marked as circles, and the values a, b, and r are taken as the maximum radius of 40 and the minimum radius of 1, based on which the circle is detected as shown in Equation 5. First, we calculated the radius using the circumference

$$C_c = (x\text{-}a)^2 + (y\text{-}b)^2 \tag{5}$$

where C_c = centre of the circle

a, b = coordinates of the centre

M-CNN was used to detect objects (pores, cracks, and fibre pullout) in the SEM images for accurate results. In M-CNN, computer vision is used to easily and accurately detect objects. It approaches the bounding objects based on the pore shape, crack shape, and fibre length. It helps to solve object detection using a convolutional neural network independently on all the regions of interest (ROI).

4. Results and Discussion

4.1 SEM images of Pineapple Leaf Fibre (PALF)

This study commenced with acquiring scanning electron microscope (SEM) images of pineapple leaf fibre (PALF), sourced from pineapple leaves. These SEM images serve as the foundational data for our automated analysis. PALF primarily consists of cellulose (70–80%),

lignin (5–12%), and ash (1.1%). Our research aligns with recent findings that advocate the use of surface-modified pineapple leaf fibres as reinforcement materials in polyester matrices. These fibres are paramount in enhancing material properties and ensuring directed learning outcomes.

4.2 Image Preprocessing and Data Collection

One of the key achievements in our methodology is the precise identification of voids within the SEM images. This was accomplished by implementing an advanced masking algorithm that employed pixel intensity thresholds, calibrated to range from 0 to 255. During this process, white and black pixels were carefully segregated. Importantly, this masking operation effectively eliminated spurious edges from the images. A total of 300 SEM image samples were systematically analysed, forming a robust dataset. This dataset was instrumental in our ability to derive meaningful insights into the SEM images and accurately predict the presence of voids and other critical features. Fig. 6 shows the original SEM images of PALF for analysis.

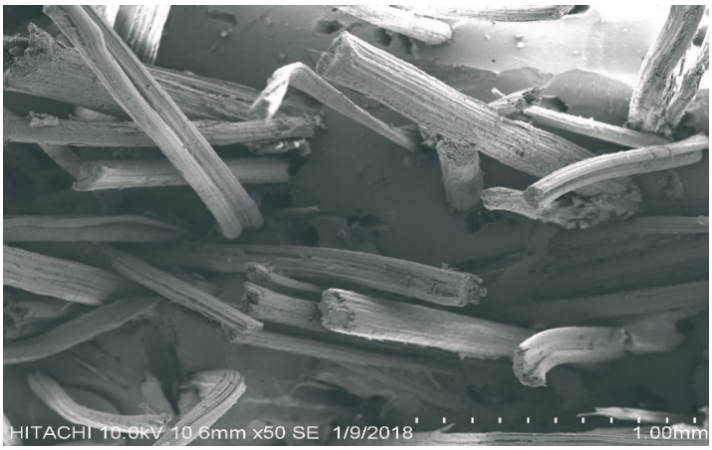

Fig. 6 Original SEM images of PALF

4.3 Voids Assessment and Evaluation

Through meticulous analysis, our algorithm facilitated the assessment of voids within the SEM images. The approach considered both pixel values and their derivatives in the image, offering a mathematical foundation for void evaluation. When pixel values were found to be independent and their derivatives increased, voids within the SEM image were accurately assessed. This quantitative output is of paramount significance as it provides researchers and professionals with a clear and comprehensive representation of voids. This knowledge, in turn, aids decision-makers in making optimal choices regarding material composition and quality.

4.4 Dataset Integrity and Segmentation

The dataset we constructed played a pivotal role in developing robust predictive models. By extracting rich, high-resolution pixel data from SEM images, we achieved remarkable fidelity to the source images. Each pixel, precisely calibrated to a range of 0 to 255, was integrated into our dataset. This dataset was subsequently employed to predict classes within new data based on pixel intensity ranges. The beauty of this approach is its ability to transcend the conventional grayscale images, providing enhanced representation through three RGB attributes. This representation allowed us to structure the classifier based on this rich information. The classifier, thus trained, facilitated precise predictions of the x and y

coordinates, resulting in highly accurate outcomes. Fig. 7 displays the detection of fibre and pore and void boundaries based on the intensity threshold.

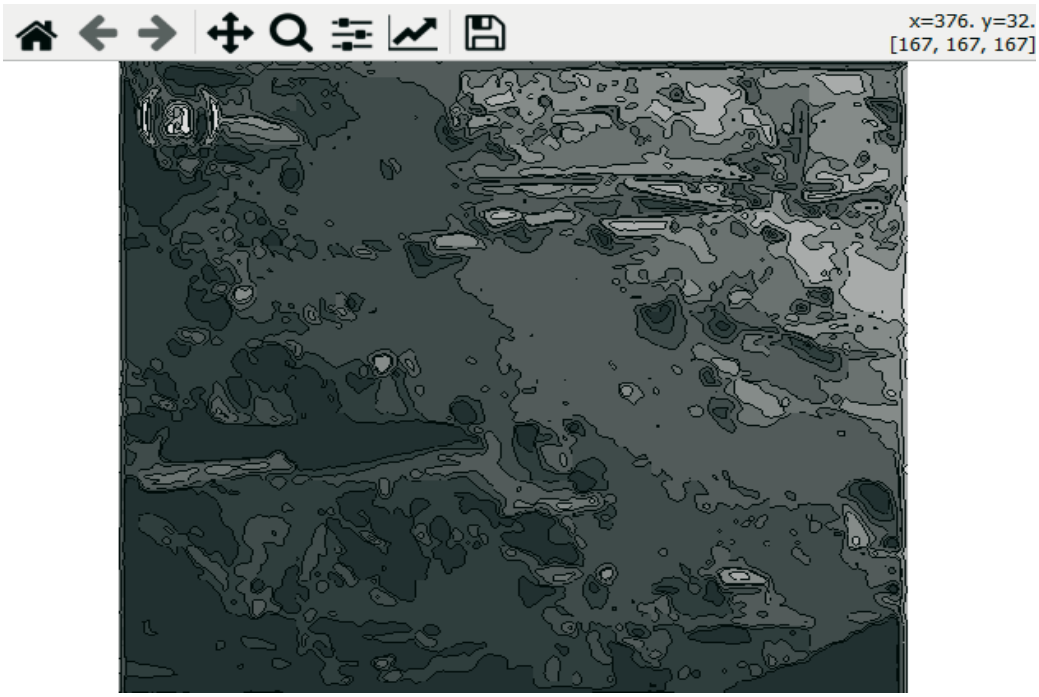

Fig. 7 Detection of fibre and pore and void boundaries using intensity threshold

4.5 Fibre Orientation, Length, and Area Analysis

The proposed methodology encompassed a comprehensive analysis of fibre properties, including orientation, length, and area. Fibre orientation was meticulously determined through mathematical concepts, dividing angles into four quadrants for precise characterisation. Such an approach allowed us to categorise fibres as ductile or brittle based on their orientation. Additionally, the statistical analysis enabled us to identify weak fibres within the composite materials, further contributing to a holistic understanding of material strength.

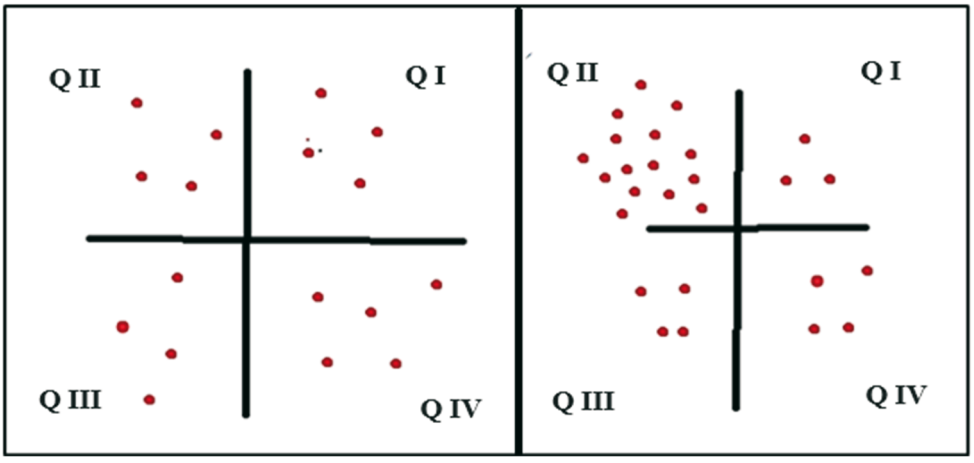

Fig. 8 Left: Voids/pores equally distributed in all four quadrants. Right: Huge voids/pores present in quadrant II

Fig. 8 shows the fibre orientation calculation. If all the fibres are equally distributed in all four quadrants, the material strength remains good. If, in any one of the four quadrants, the fibres are bulked, the material has huge voids/pores and cracks and therefore the material is weak.

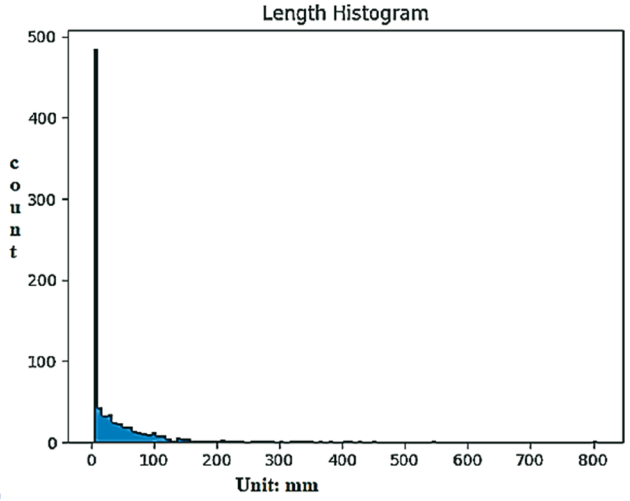

Fig. 9 Measurement of fibre length in SEM images

Fig. 9 shows the histogram of the fibre length measurement from the SEM images. Moreover, our automated software exhibited the capability to compute fibre length in micrometres (μm) with remarkable accuracy. This analysis involved evaluating the statistical distribution of fibre diameters, enabling the software to distinguish genuine fibres from spurious ones. The output, provided in μm, ensured reliable and reproducible measurements of fibre length, surpassing the capabilities of manual analysis.

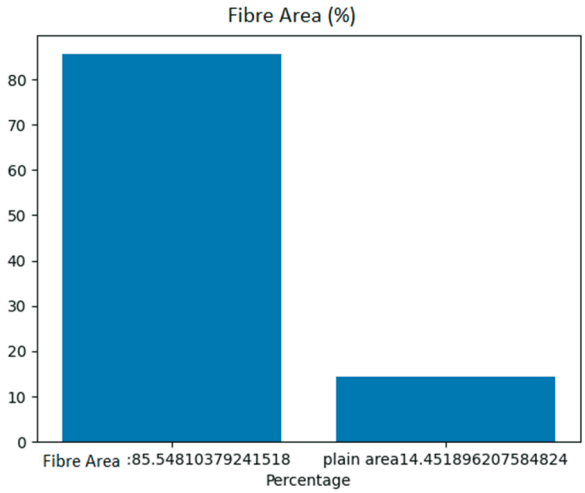

Fig. 10 Estimation of fibre area as a percentage

In terms of the fibre area estimation, our software dynamically calculated the total area occupied by fibres within the SEM images as a percentage, as shown in Fig. 10. By considering the presence of fibres, cracks, and voids, the software discerned plain areas where these features were absent. The SEM image demonstrates that the fibre area comprises 85.54% of the total area, while the plain area accounts for 14.45%. This quantitative analysis is critical for determining the amount of fibre area present in the SEM images.

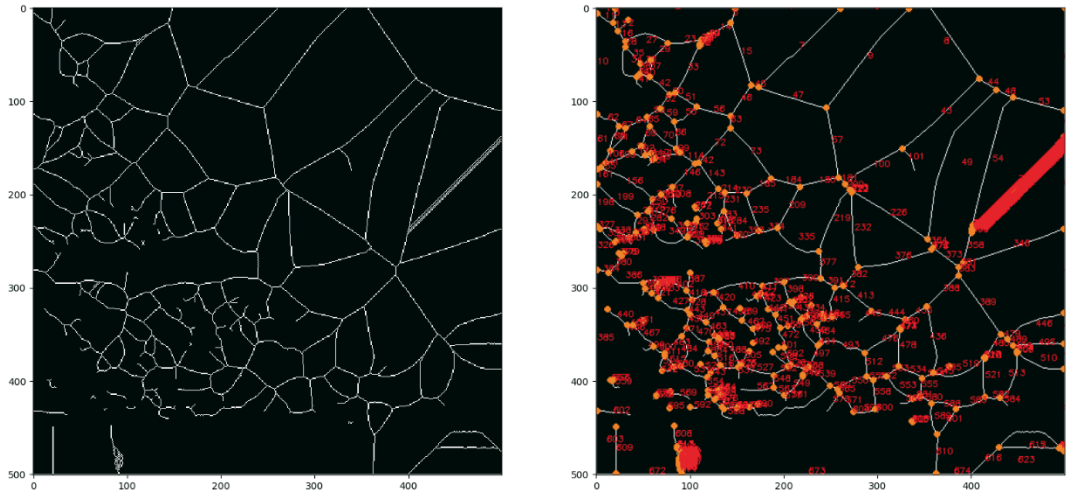

Fig. 11 Prediction of fibre angle orientation in SEM Images

The orientation of the fibre determines the strength of the material. The orientation was calculated based on the angle measurement where it is divided into four quadrants. The proposed automated software employed with M-CNN fixed the 1st quadrant angle at 0 to 90 degrees. The 2nd quadrant angle is 90 to 180 degrees. The 3rd quadrant angle is 180 to 270 degrees. The 4th quadrant is 270 to 360 degrees. Fig. 11 shows the prediction of angle orientation for the fibres.

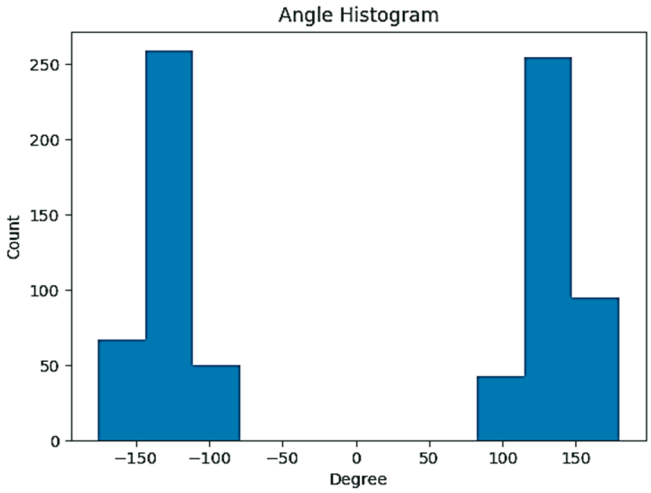

Fig. 12 Statistical analysis of fibre angle orientation

The proposed automated software M-CNN predicted the angle distribution of all fibres present in the SEM images where it set 45° as ductile and 90° as brittle. Fig. 12 clearly represents the fibre angle orientation. The position of individual fibres is measured accurately, and their angle is measured statistically. Finding the orientation is a crucial factor in determining the tensile strength. By using this technique, the fibre orientation and strength of the material can be determined effectively.

4.6 Crack and Void Detection

The proposed software, driven by M-CNN, excelled in predicting cracks and voids, even at a minute scale. Fig. 13 provides a visual representation of this achievement. The capability to detect and quantify these features outperformed manual observation, reinforcing the reliability of our approach.

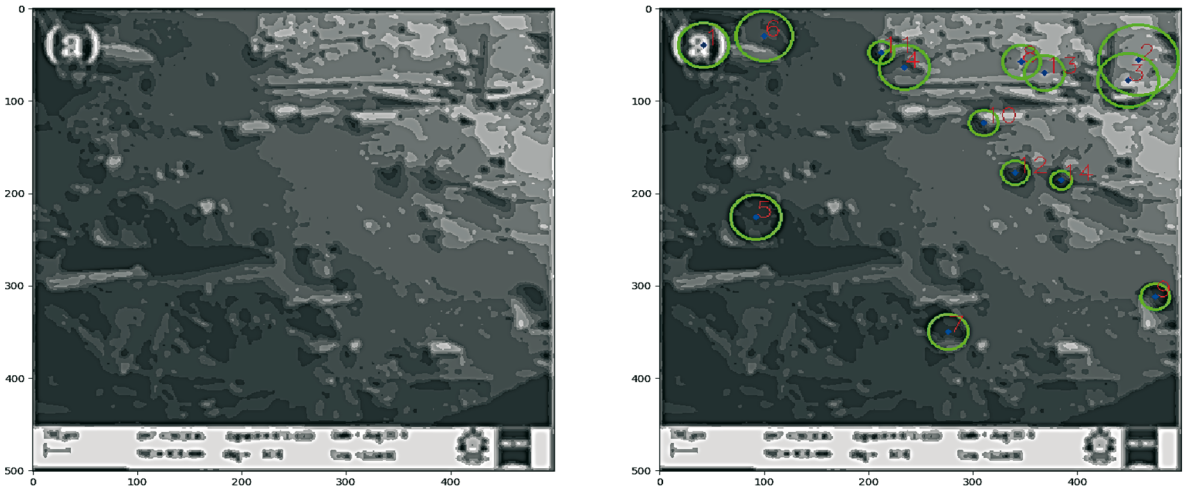

Fig. 13 Left: Analysis of pores/voids in SEM images. Right: Prediction of cracks encircled in SEM images

4.7 Diameter Calculation and 3D Visualisation

Using mathematical calculations, the software accurately calculated the diameter of both pores and cracks, contributing to a quantitative assessment of these critical features.

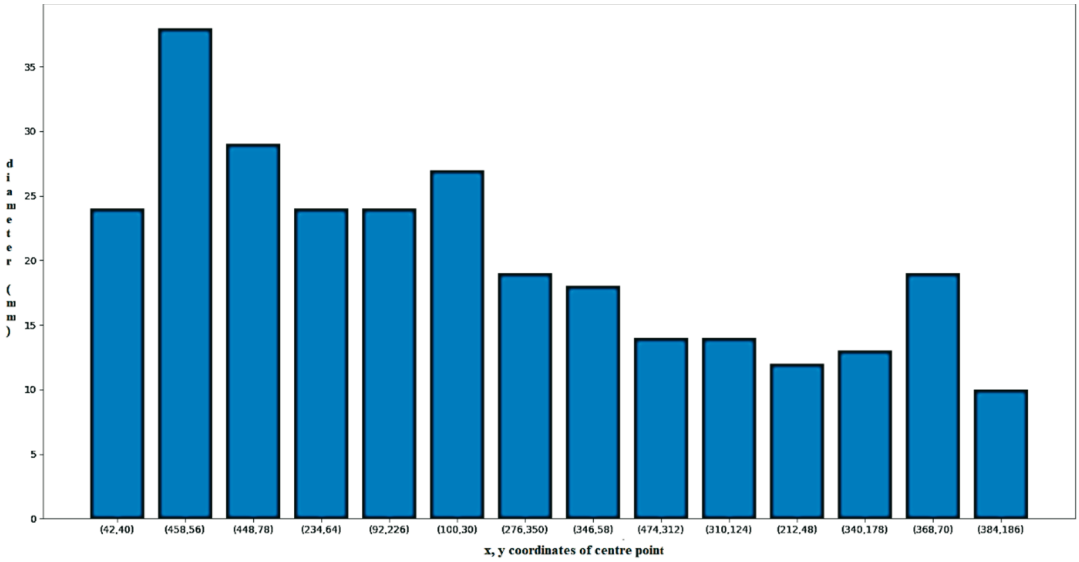

Fig. 14 Calculation of the diameter of pores/voids and cracks using the proposed automated software

The M-CNN applied Equation (3) in the calculation of the diameter of the pores and the cracks which is shown in Fig. 14. The diameter of the pores can be easily calculated using statistical analysis. The midpoint of the x and y coordinates helps in finding the radius of the circle. In the XY plane, two ordered pairs are used to find the distance of the pores and cracks. The midpoint coordinates (x and y) facilitated a precise determination of the radius, thus ensuring robust measurements.

Additionally, the proposed approach extended to 3D visualisation, enhancing the understanding of fibre distribution and enabling a precise coordination of various elements within the SEM images. Fig. 15 presents an overview of the fibre distribution in the 3D analysis. The 3D result depicted offers an enriched perspective of fibre distribution within the original SEM image. It enhances the interpretation by providing the spatial context, revealing patterns, and allowing for a more intuitive understanding of fibre arrangements. This result contributes

to improved understanding, aiding researchers in identifying trends and irregularities. Additionally, the 3D analysis facilitates the precise coordination of various elements, such as fibres, pores, and cracks, contributing to material integrity.

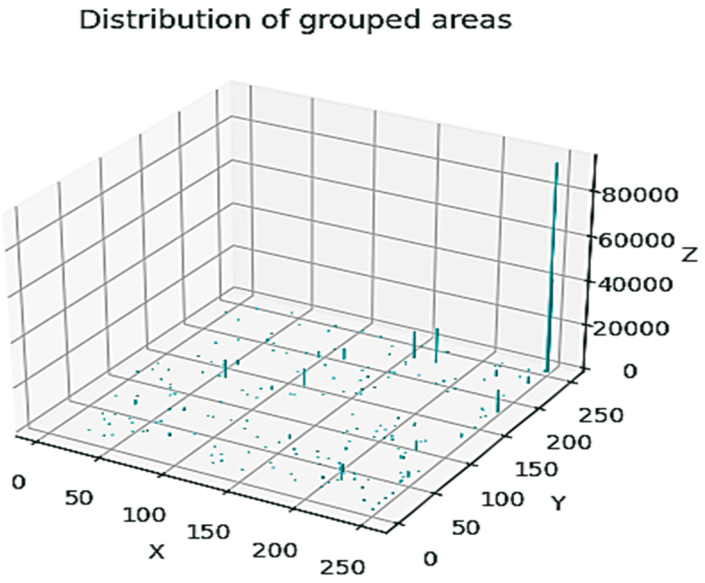

Fig. 15 Distribution of fibres in a 3D view

4.8 Accuracy and Efficiency

The performance of the proposed software was benchmarked in terms of accuracy and processing time. As demonstrated in Fig. 16, the software achieved an impressive accuracy rate of 99% in predicting fibre orientation, cracks, and voids within SEM images, surpassing conventional CNN methods by a significant margin. Furthermore, our software demonstrated remarkable efficiency, completing the analysis in a significantly shorter timeframe (15,000 ms compared to 21,000 ms), further emphasising its superiority.

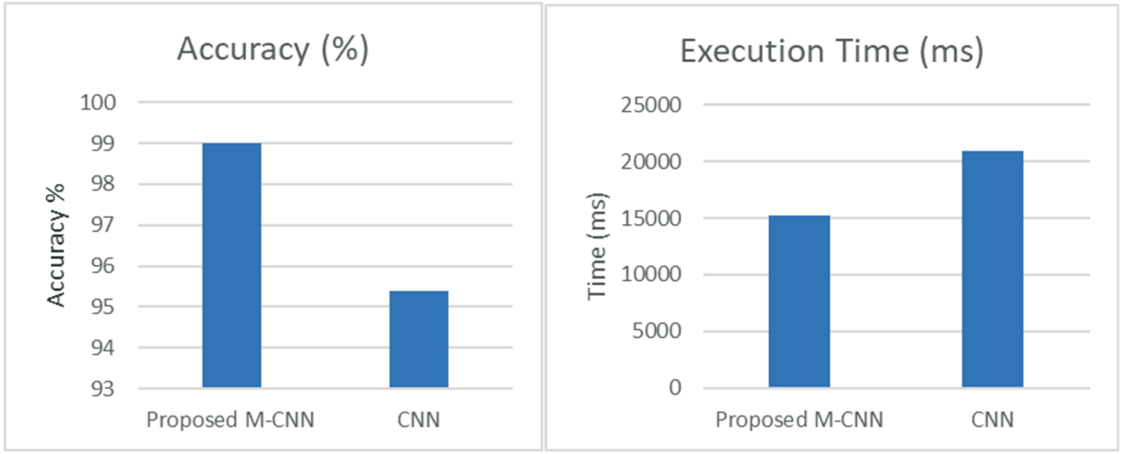

Fig. 16 Determination of accuracy and time of the proposed software

This study has resulted in the development of advanced automated software, powered by M-CNN, which significantly enhances our ability to assess material strength in fibre composite SEM images. The software offers researchers and professionals a comprehensive toolkit to analyse various parameters qualitatively and quantitatively. It empowers decision-makers to make informed choices regarding material composition, quality, and performance, ultimately

advancing the field of material science. Future developments in this work are expected to integrate Artificial Neural Networks (ANN) and Recurrent Neural Networks (RNN) to further enhance the capabilities and applications of our automated software.

The Results of Illustrative Examples

In our proposed work, some more examples are shown in Fig. 17 for calculating the voids, cracks, and orientation of the SEM images. The proposed work is suitable for all the same images and it predicts the length of fibre, cracks in the fibre, the measurement of cracks in diameter, and estimates the fibre area and fibre angle statistically. Our automated software helps in predicting the material strength of fibre in the SEM images.

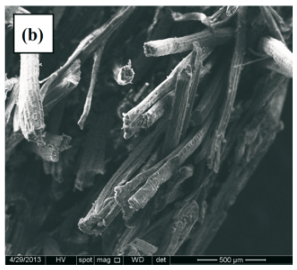

Original SEM image

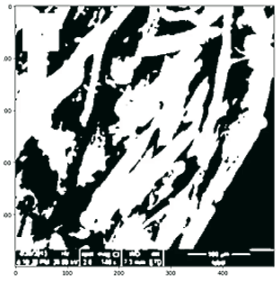

Detection of fiber, pore and void boundaries using intensity threshold

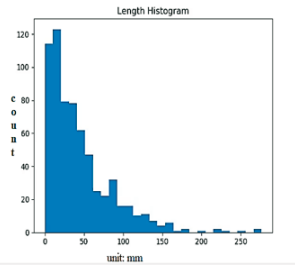

Measurement of Fiber Length present in SEM images

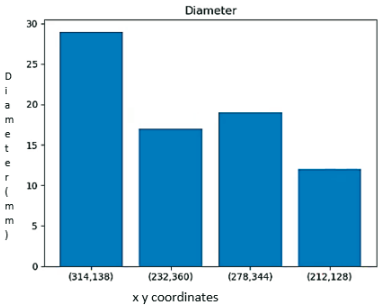

Calculation of diameter of pores/voids and cracks using proposed automated software

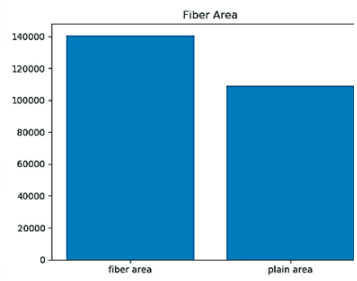

Estimation of fiber area

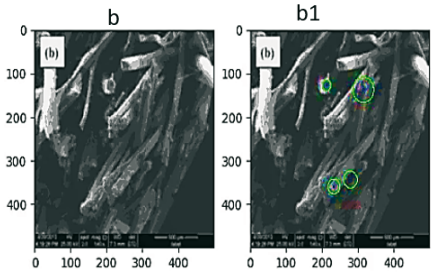

Figure (b) Analysis of pores/voids in SEM images
Figure (b1) Prediction of cracks in diameter of SEM images

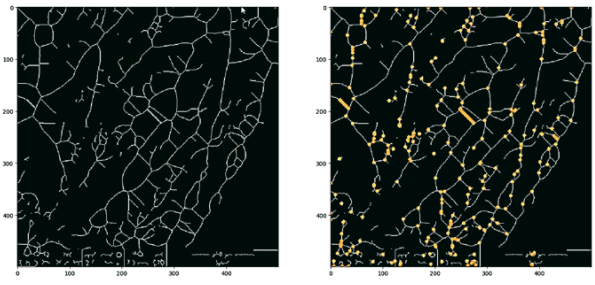

Prediction of fiber angle orientation in SEM Images

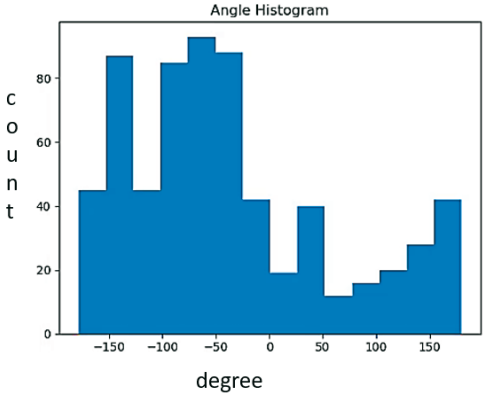

Statistical analysis of fiber angle orientation

Fig. 17 Additional illustrative examples developed by the M-CNN algorithm

5. Conclusion

In this study, we have presented a comprehensive analysis of Pineapple Leaf Fiber (PALF) SEM images, employing advanced image processing techniques and a Convolutional Neural Network (CNN) architecture known as the Mask Convolutional Neural Network (M-

CNN). Our research has contributed significant findings in the field of material science and automated image analysis.

Our automated software, driven by M-CNN, has proven to be a powerful tool for evaluating the material strength of fibre composite SEM images. We have achieved several noteworthy outcomes and insights:

1. Precise voids assessment: through advanced masking techniques and pixel intensity thresholds, we have successfully identified and quantified voids in SEM images. This quantitative approach provides valuable data for material composition analysis and quality control.
2. A rich and reliable dataset: our construction of a dataset, comprising 300 SEM image samples, has played a pivotal role in developing accurate predictive models. This dataset, characterised by high-resolution pixel data, ensures fidelity to the source images and enables robust predictions.
3. Comprehensive fibre analysis: our methodology has enabled a comprehensive analysis of fibre properties, including orientation, length, and area. The software's ability to categorise fibres based on orientation and to accurately compute fibre length in micrometres has advanced our understanding of material strength.
4. Effective crack and void detection: our software has excelled in detecting cracks and voids, even at a minute scale, surpassing manual observation. This capability enhances our ability to assess material quality and structural integrity.
5. Accurate diameter calculations: utilizing mathematical calculations, our software has accurately determined the diameter of pores and cracks, providing quantitative insights into these critical features.
6. Efficiency and accuracy: our proposed software has demonstrated remarkable efficiency, completing analyses in significantly shorter timeframes compared to conventional CNN methods while achieving an impressive accuracy rate of 99%.

This research has introduced a powerful and versatile tool for material scientists and professionals. The automated software, based on M-CNN, empowers users to qualitatively and quantitatively analyse fibre composite SEM images, facilitating informed decision-making regarding material composition, quality, and performance. This work represents a significant step forward in the field of material science and sets the stage for future developments, including the integration of Artificial Neural Networks (ANN) and Recurrent Neural Networks (RNN), which promise to further enhance the capabilities and applications of our automated software. These findings underscore the potential of automated image analysis in material science, offering new avenues for research and development in this vital field. As technology continues to advance, we expect even more sophisticated tools and methodologies, ultimately contributing to the continued evolution of material science and its diverse applications.

REFERENCES

[1] F. Kruggel, A simple measure for acuity in medical images, IEEE Trans. Image Proc. 27 (11) (2018), 5225-5233. https://doi.org/10.1109/TIP.2018.2851673

[2] A.H. Abdel-Gawad, L.A. Said, A.G. Radwan, Optimized edge detection technique for brain tumor detection in MR images, IEEE Access 8 (2020) 136243-136259. https://doi.org/10.1109/ACCESS.2020.3009898

[3] W. Yang, L. Zhong; Y. Chen, L. Lin, Z. Lu, S. Liu, Y. Wu, Q. Feng, W. Chen, Predicting CT image from MRI data through feature matching with learned nonlinear local descriptors, IEEE Trans. Med. Image 37 (4) (2018) 977-987. https://doi.org/10.1109/TMI.2018.2790962

[4] Y. Li, D. Liu, H. Li, L. Li, Z. Li, F. Wu, Learning a convolutional neural network for image compact-resolution, IEEE Trans. Image Proc. 28 (3) (2019) 1092-1107. https://doi.org/10.1109/TIP.2018.2872876

[5] Wei Jia, Mingshan Xie, An Efficient License Plate Detection Approach with Deep Convolutional Neural Networks in Unconstrained Scenarios, IEEE Access, Volume: 11, 2023. https://doi.org/10.1109/ACCESS.2023.3301122

[6] Zhong, Q., Chen, Y., Zhu, B., Liao, S., & Shi, K. (2022). A temperature field reconstruction method based on acoustic thermometry. Measurement, 200, 111642. https://doi.org/10.1016/j.measurement.2022.111642

[7] Huang, Z., Luo, P., Wu, Q., & Zheng, H. (2022). Constructing one-dimensional mesoporous carbon nanofibers loaded with NaTi2(PO4)3 nanodots as novel anodes for sodium energy storage. Journal of Physics and Chemistry of Solids, 161, 110479. https://doi.org/10.1016/j.jpcs.2021.110479

[8] Jiang, W., Ren, T., & Fu, Q. (2024). Deep Learning in the Phase Extraction of Electronic Speckle Pattern Interferometry. Electronics, 13(2), 418. https://doi.org/10.3390/electronics13020418

[9] Liao, D., Zhu, S., Keshtegar, B., Qian, G., & Wang, Q. (2020). Probabilistic framework for fatigue life assessment of notched components under size effects. International Journal of Mechanical Sciences, 181, 105685. https://doi.org/10.1016/j.ijmecsci.2020.105685

[10] Niu, X., Zhu, S., He, J., Liao, D., Correia, J. A. F. O., Berto, F., Wang, Q. (2022). Defect tolerant fatigue assessment of AM materials: Size effect and probabilistic prospects. International Journal of Fatigue, 160, 106884. https://doi.org/10.1016/j.ijfatigue.2022.106884

[11] Dong, Y., Xu, B., Liao, T., Yin, C., & Tan, Z. (2023). Application of Local-Feature-Based 3-D Point Cloud Stitching Method of Low-Overlap Point Cloud to Aero-Engine Blade Measurement. IEEE Transactions on Instrumentation and Measurement, 72. https://doi.org/10.1109/TIM.2023.3309384

[12] Shi, Y., Xi, J., Hu, D., Cai, Z., & Xu, K. (2023). RayMVSNet++: Learning Ray-Based 1D Implicit Fields for Accurate Multi-View Stereo. IEEE Transactions on Pattern Analysis and Machine Intelligence, 45(11), 13666-13682. https://doi.org/10.1109/TPAMI.2023.3296163

[13] Jiongyi Yan, Emrah Demirci, Andrew Gleadall, 3D short fiber orientation for universal structures and geometries in material extrusion additive manufacturing, Additive Manufacturing, Volume 69, 2023. https://doi.org/10.1016/j.addma.2023.103535

[14] Zhenghao Li, Jiajia Zhou, Christopher K.Y. Leung, Fiber orientation distribution in strain hardening cementitious composites (SHCC): Experimental investigation and consideration of processing effect, Cement and Concrete Research, Volume 170, 2023. https://doi.org/10.1016/j.cemconres.2023.107190

[15] Celine Lauff, Matti Schneider, John Montesano, Thomas Böhlke, An orientation corrected shaking method for the microstructure generation of short fiber-reinforced composites with almost planar fiber orientation, Composite Structures, Volume 322, 2023. https://doi.org/10.1016/j.compstruct.2023.117352

[16] Vaishakh Raju, Poornesh Kumar Koorata, Computational assessment on the impact of collagen fiber orientation in cartilages on healthy and arthritic knee kinetics/kinematics, Medical Engineering & Physics, Volume 117, 2023. https://doi.org/10.1016/j.medengphy.2023.103997

[17] Bi Weihong; Jin Yun; Li Jiaxin; Sun Lingling; Fu Guangwei; Jin Wa, In-Situ Detection Method of Jellyfish Based on Improved Faster R-CNN and FP16, IEEE Access, Volume: 11, 2023. https://doi.org/10.1109/ACCESS.2023.3300655

[18] Hajer Khachnaoui; Belkacem Chikhaoui; Nawres Khlifa; Rostom Mabrouk, Enhanced Parkinson's Disease Diagnosis Through Convolutional Neural Network Models Applied to SPECT DaTSCAN Images, IEEE Access, Volume: 11, 2023. https://doi.org/10.1109/ACCESS.2023.3308075

[19] Yuanxin Ye; Mengmeng Wang; Liang Zhou; Guangyang Lei; Jianwei Fan; Yao Qin, Adjacent-Level Feature Cross-Fusion With 3-D CNN for Remote Sensing Image Change Detection, IEEE Transactions on Geoscience and Remote Sensing, Volume: 61, 2023. https://doi.org/10.1109/TGRS.2023.3305499

[20] Seunghwan Song; Bosung Jeon; Munhyeon Kim; Jae-Joon Kim, Efficient Convolutional Processing of Spiking Neural Network with Weight-Sharing Filters, IEEE Electron Device Letters, Vol. 44, Issue: 6, pp: 1007 - 1010, 2023. https://doi.org/10.1109/LED.2023.3265065

[21] Ding, H., Gong, P., Chen, W., Peng, Z., Bu, H., Zhang, M., Schroers, J. (2023). Achieving strength-ductility synergy in metallic glasses via electric current-enhanced structural fluctuations. International Journal of Plasticity, 169, 103711. https://doi.org/10.1016/j.ijplas.2023.103711

[22] Shen, Z., Dong, R., Li, J., Su, Y., & Long, X. (2024). Determination of gradient residual stress for elastoplastic materials by nanoindentation. Journal of Manufacturing Processes, 109, 359-366. https://doi.org/10.1016/j.jmapro.2023.10.030

[23] Su, Y., Shen, Z., Long, X., Chen, C., Qi, L., Chao, X. (2023). Gaussian filtering method of evaluating the elastic/elasto-plastic properties of sintered nanocomposites with quasi-continuous volume distribution. Materials Science and Engineering: A, 872, 145001. https://doi.org/10.1016/j.msea.2023.145001

[24] Lianlin Li; Long Gang Wang; Fernando L. Teixeira, Performance Analysis and Dynamic Evolution of Deep Convolutional Neural Network for Electromagnetic Inverse Scattering, IEEE Antennas and Wireless Propagation Letters, Volume: 18, Issue: 11, pp: 2259 - 2263, 2019. https://doi.org/10.1109/LAWP.2019.2927543

[25] Juanjuan Huang; Sai Huang; Yuqi Zeng; Hao Chen; Shuo Chang; Yifan Zhang, Hierarchical Digital Modulation Classification Using Cascaded Convolutional Neural Network, Journal of Communications and Information Networks, Volume: 6, Issue: 1, pp: 72 - 81, 2021 https://doi.org/10.23919/JCIN.2021.9387706

[26] Pengbo Zhang, Xue Wang, Weihang Zhang, Junfeng Chen, Learning Spatial-Spectral-Temporal EEG Features with Recurrent 3D Convolutional Neural Networks for Cross-Task Mental Workload Assessment, IEEE Transactions on Neural Systems and Rehabilitation Engineering (2019) https://doi.org/10.1109/TNSRE.2018.2884641

[27] Zheng Liu, Botao Xiao, Muhammad Alrabeiah, Keyan Wang, Jun Chen "Single Image Dehazing with a Generic Model-Agnostic Convolutional Neural Network" IEEE Signal Processing Letters (2019). https://doi.org/10.1109/LSP.2019.2910403

[28] Mridul Gupta; Jonathan Chan; Mitchell Krouss; Greg Furlich; Paul Martens; Moses W. Chan; Mary L. Co, Infrared Small Target Detection Enhancement Using a Lightweight Convolutional Neural Network, IEEE Geoscience and Remote Sensing Letters, Volume: 19, 2022. https://doi.org/10.1109/LGRS.2022.3203931

[29] Berin Šeta, Michael Sandberg, Marco Brander, Md Tusher Mollah, Deepak Pokkalla, Vipin Kumar, Jon Spangenberg, Modeling fiber orientation and strand shape morphology in three-dimensional material extrusion additive manufacturing, Composites Part B: Engineering, Volume 266, 2023. https://doi.org/10.1016/j.compositesb.2023.110957

[30] Haramina, T., Fulanović, L., & Macan, J. (2019). Effect of Weathering on Dynamic Mechanical Properties of the Multilayer Polyamide//Ethylene Vinyl Alcohol Copolymer//Polyamide//Polyethylene Film. Transactions of FAMENA, 43(4), 1-16. https://doi.org/10.21278/TOF.43401

[31] Hrman, D., Rakvin, M., & Markučić, D. (2013). Optimization of scanning parameters of computed radiography for characterization of expanded polystyrene. Transactions of FAMENA, 37(3), 53-64.

[32] Kumar, R., Chattopadhyaya, S., Ghosh, A., Krolczyk, G. M., Vilaca, P., Kumar, R., ... & Triphathi, R. (2017). Characterization of friction surfaced coatings of AISI 316 tool over high-speed-steel substrate. Transactions of FAMENA, 41(2), 61-76. https://doi.org/10.21278/TOF.41206

[33] Zhang, W., Kang, S., Liu, X., Lin, B., & Huang, Y. (2023). Experimental study of a composite beam externally bonded with a carbon fiber-reinforced plastic plate. Journal of Building Engineering, 71, 106522. https://doi.org/10.1016/j.jobe.2023.106522

[34] Fu, C., Yuan, H., Xu, H., Zhang, H., & Shen, L. (2023). TMSO-Net: Texture adaptive multi-scale observation for light field image depth estimation. Journal of Visual Communication and Image Representation, 90, 103731. https://doi.org/10.1016/j.jvcir.2022.103731

[35] Zhang, C., Khorshidi, H., Najafi, E., & Ghasemi, M. (2023). Fresh, mechanical and microstructural properties of alkali-activated composites incorporating nanomaterials: A comprehensive review. Journal of Cleaner Production, 384, 135390. https://doi.org/10.1016/j.jclepro.2022.135390

[36] Zhihao Li, Wei Zhou, Tensile behavior of UHPFRC made by a fiber orientation device with adjustable vibrational frequency, Construction and Building Materials, Volume 401, 2023. https://doi.org/10.1016/j.conbuildmat.2023.132914

[37] Matteo Giardino, Devanarayanan Meena Narayana Menon, Davide Luca Janner, Regularization techniques for 3D surface reconstruction from four quadrant backscattered electron detector images, Ultramicroscopy, Volume 250, August 2023. https://doi.org/10.1016/j.ultramic.2023.113746

[38] Kan, Y., Kan, H., Bai, Y., Zhang, S., & Gao, Z. (2023). Effective and environmentally safe self-antimildew strategy to simultaneously improve the mildew and water resistances of soybean flour-based adhesives. Journal of Cleaner Production, 392, 136319. https://doi.org/10.1016/j.jclepro.2023.136319

[39] Jia, L., Wang, Z., Wang, L., Zeng, J., Du, P., Yue, Y., Jia, S. (2023). Self-standing boron nitride bulks enabled by liquid metals for thermal management. Materials Horizons, 10(12), 5656-5665. https://doi.org/10.1039/D3MH01359F

[40] Tian, G., Hui, Y., Lu, W., & Tingting, W. (2023). Rate-distortion optimized quantization for geometry-based point cloud compression. Journal of Electronic Imaging, 32(1), 13047. https://doi.org/10.1117/1.JEI.32.1.013047

[41] Xing, J., Yuan, H., Hamzaoui, R., Liu, H., & Hou, J. (2023). GQE-Net: A Graph-Based Quality Enhancement Network for Point Cloud Color Attribute. IEEE Transactions on Image Processing, 32, 6303-6317. https://doi.org/10.1109/TIP.2023.3330086

[42] S.L. Lu, D. Han, D.Y. Qin, T. Song, D. Qiu, M. Brandt, H.P. Tang, M. Qian, Massive transformations in titanium alloys: Role of relative orientation of adjacent parent grains, Volume 239, 15 January 2024. https://doi.org/10.1016/j.scriptamat.2023.115776

[43] Hyeon-Gyu Min, Jun-Hyub Park, Development of in-situ SEM testing apparatus for observing behavior of material at high magnification during tensile test, Measurement, Volume 221, 2023. https://doi.org/10.1016/j.measurement.2023.113454

[44] Peter Guenther, Miriam Guenther, Christian M. Ringle, Ghasem Zaefarian, Severina Cartwright, Improving PLS-SEM use for business marketing research, Industrial Marketing Management, Volume 111, 2023. https://doi.org/10.1016/j.indmarman.2023.03.010

[45] Dejun Xi; Yi Qin; Jun Luo; Huayan Pu; Zhiwen Wang, Multipath Fusion Mask R-CNN With Double Attention and Its Application into Gear Pitting Detection, IEEE Transactions on Instrumentation and Measurement, Volume: 70, 2021. https://doi.org/10.1109/TIM.2021.3049276

[46] Hyeseung Park; Seungchul Park; Youngbok Joo, Detection of Abandoned and Stolen Objects Based on Dual Background Model and Mask R-CNN, IEEE Access, Volume: 8, 2020. https://doi.org/10.1109/ACCESS.2020.2990618

[47] Lento Manickathan, Claudio Mucignat and Ivan Lunati, Kinematic training of convolutional neural networks for particle image velocimetry, Volume 33, Measurement Science and Technology, 2022. https://doi.org/10.1088/1361-6501/ac8fae

[48] Ping Ma1, Hongli Zhang, Wenhui Fan2, Cong Wang, Guangrui Wen and Xining Zhang, A novel bearing fault diagnosis method based on 2D image representation and transfer learning-convolutional neural network, Volume 30, Measurement Science and Technology, 2019. https://doi.org/10.1088/1361-6501/ab0793

[49] Jianhui Yang and Zhenrui Peng, A new convolutional neural network-based framework and data construction method for structural damage identification considering sensor placement, Volume 34, Measurement Science and Technology, 2023. https://doi.org/10.1088/1361-6501/acc755

[50] Srikanth Sagar Bangaru, Chao Wang, Xu Zhou, Marwa Hassan, scanning electron microscopy (SEM) image segmentation for microstructure analysis of concrete using U-net convolutional neural network, Automation in Construction, Volume 144, 2022. https://doi.org/10.1016/j.autcon.2022.104602

Submitted: 28.10.2023

Accepted: 15.4.2024

Ganesan Elizabeth Rani*
Department of Artificial Intelligence and Data Science, KIT-Kalaignarkarunanidhi Institute of Technology, Coimbatore-641 402, Tamil Nadu, India
Marimuthu Sakthimohan
Department of Electronics and Communication Engineering , KIT-Kalaignarkarunanidhi Institute of Technology, Coimbatore-641 402, Tamil Nadu, India
Arockiasamy Felix Sahayaraj
Department of Mechanical Engineering, KIT-Kalaignarkarunanidhi Institute of Technology, Coimbatore-641 402, Tamil Nadu, India
Mariappan Sornalakshmi
Department of Computer Science PG, Arulmigu Kalasalingam College of Arts and Science, Krishnan Kovil-626 126, Tamil Nadu, India
*Corresponding author:
kit.elizabethrani@gmail.com